Optic Nerve involvement in Experimental Autoimmune Encephalomyelitis to homologous Spinal Cord Homogenate immunization in the Dark Agouti rat

Valerio Castoldi [1], Silvia Marenna[2], Roberto Santangelo[2,] Raffaele d'Isa[1], Marco Cursi[3], Linda Chaabane[1], Angelo Quattrini[1], Giancarlo Comi[1,2], Letizia Leocani[1,2]

[1]San Raffaele Scientific Institute, Division of neuroscience - INSPE - Institute of Experimental Neurology, Experimental neurophysiology

[2]Vita-Salute San Raffaele University

[3]San Raffaele Scientific Institute, Neurology Area

Introduction

Experimental autoimmune encephalomyelitis (EAE) is the most common preclinical model for multiple sclerosis (MS), characterized by inflammation, demyelination, axonal loss and gliosis[1]. EAE can be actively induced by immunization with several myelin peptides, as well as with CNS-derived tissues, like spinal cord homogenate (SCH) derivates[2]. The Dark Agouti (DA) rat strain immunized with SCH develops a protracted and relapsing EAE[3]. Although motor symptoms have already been studied in this MS model[4], little is known about central nervous system damage, in particular what happens in visual pathways. We will focus our investigation in this district, since visual symptoms are common in MS patients[5]. In particular, we explored the involvement of visual pathways in SCH-EAE using VEPs, which are reliable biomarkers of neurophysiological dysfunctions affecting optic nerves (ONs)[6]. In this work, VEPs were recorded with two different methods, using epidural screw or epidermal cup electrodes. This last procedure showed statistically equivalent latencies compared to the classic epidural-implanted electrodes, avoids surgery and allows longer follow-up studies[7]. In order to investigate what happens in later stages of SCH-EAE, the epidermal-recorded rats were monitored for three additional weeks with respect to implanted rats. Together with VEPs, the EAE rats were monitored by checking motor signs. At the end of the study we performed histological analysis of ONs.

Methods

Animals

Twenty-seven (n = 27) female DA rats, 8 weeks aged, with a body weight of 110-130 g were used in these experiments.

Experimental protocol

Baseline VEPs were recorded through epidural screw or epidermal cup electrodes in 27 DA rats. EAE was induced in 12 rats through injection of rat SCH at the base of the tail. EAE motor symptoms were assessed daily, while VEPs were recorded once a week for five (**Fig 1**) or eight weeks (**Fig 2**) with epidural (n = 14, 6 immunized) and epidermal (n = 13, 6 immunized) electrodes, respectively. At the end of the study, ON histopathology was performed.

Clinical assessment of EAE rats

Clinical profile was daily followed from 0 to 21 days post immunization (dpi). Clinical score ranged from 0 to 5 (0: no symptoms; 0.5: tail weakness; 1: complete tail paralysis; 1.5: complete tail paralysis and weakness of the hind limbs 2: complete tail paralysis and pronounced weakness of the hind limbs; 2.5: hind limbs do not support the body weight, but without complete paralysis; 3: complete paralysis of the hind limbs; 3.5: complete paralysis of the hind limbs and partial paralysis of front paws; 4: complete paralysis of front and hind paws; 5: death due to the severity of the clinical symptoms.

VEP recording

Flash VEPs from right eyes were recorded under sevoflurane anesthesia (2 - 2.5%) using epidural screw electrodes or 6 mm Ø Ag/Cl cup scalp electrodes over the contralateral primary visual cortex, with a reference needle electrode inserted in the nose. For each VEP session, the average of 4 waveforms (10 flashes each) was used for measuring the latency (expressed in ms) of N1 from the complex P1-N1-P2 of flash-VEPs[8].

Histology

ONs emerging from right eyes were fixed in 2% buffered glutaraldehyde and post-fixed in 1% osmium tetroxide. After alcohol dehydration, these samples were embedded in Epon (Fluka™). Transverse sections (0.5–1 pm thick) were stained with toluidine blue and examined by light microscopy. To evaluate ON pathological areas, a quantitative analysis was performed with ImageJ software on 100× digital images. Damaged areas were manually selected, measured and normalized on the total ON area.

Statistical analysis

Clinical scores were analyzed through Friedman test followed by Dunn post-hoc test. N1 latency mean values from H and EAE groups were compared using two-way ANOVA for repeated measures with "time" as "within subjects" main factor and "disease" as "between subjects" main factor, followed by LSD post-hoc test. Histological differences between H and EAE ONs were compared using Welch t-test for heteroscedastic samples. Data were considered significant at p < .05.

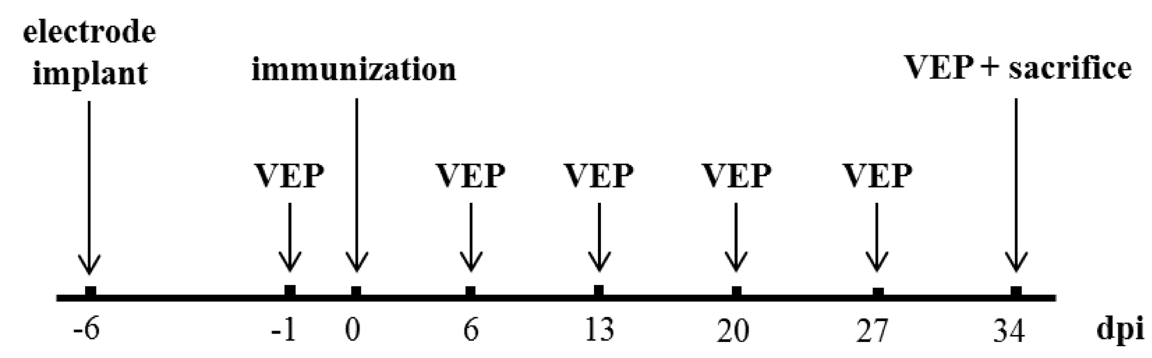

Figure 1. Experimental design of the study with epidural-recorded rats.

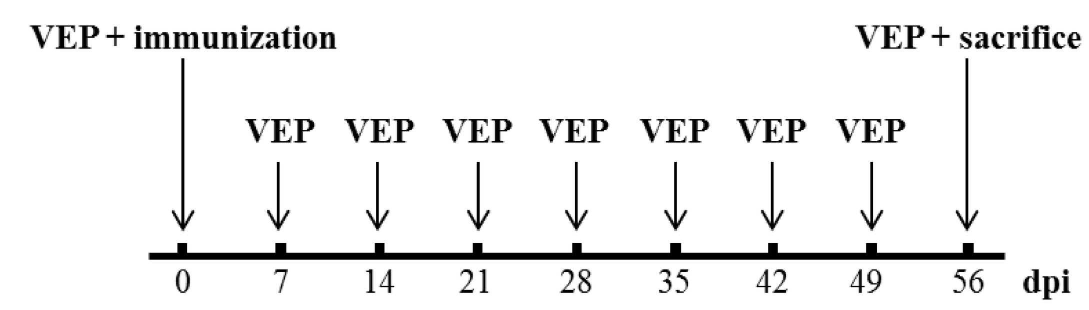

Figure 2. Experimental design of the study with epidermal-recorded rats.

Results

Clinical assessment of EAE

In implanted EAE rats, the disease onset ranged from 6 to 9 dpi. Total remission was observed in 4 out of 6 rats (66.7%) and occurred between 20 and 32 dpi. Relapses were seen in 3 rats (50%), while EAE signs were chronic in 2 rats (33.3%), persisting until sacrifice (**Fig 3A**). The totality of implanted EAE rats showed clinical symptoms between 9 and 19 dpi, whereas the minimal percentage of diseased animals (33.3%) was observed from 32 to 34 dpi (**Fig 3B**). Considering the mean clinical score of implanted rats (**Fig 3C**), the first disease peak was detected at 10 dpi. Compared with the first peak of the disease, the clinical score significantly decreased from 20 to 27 dpi (first remission, 20 dpi: p = .007; 21 and 22 dpi: p < .0001; 23 dpi: p = .007; from 24 to 26 dpi: p < .05), then this reduction was no longer significant at 27 dpi (relapse phase), returning significant from 28 to 34 dpi (second remission, 28 dpi: p = .019; from 29 to 34 dpi: p < .01). In non-implanted EAE rats, the disease onset ranged from 7 to 11 dpi. Total remission was observed in 4 out of 6 rats (66.7%) and occurred between 22 and 27 dpi. Relapses were seen in 4 rats (66.7%), while EAE signs were chronic in 2 rats (33.3%), enduring until sacrifice (**Fig 4A**). The totality of non-implanted EAE rats showed clinical symptoms between 11 and 15 dpi, whereas the minimal percentage of diseased animals (33.3%) was observed from 27 to 56 dpi (**Fig 4B**). Considering the mean clinical score of non-implanted rats (**Fig 4C**), the first disease peak was detected at 13 dpi. With respect to the first peak of the disease, the clinical score significantly decreased at 20 and 21 dpi (first remission, 20 dpi: p = .024; 21 dpi: p = .012), then this reduction was no longer significant from 22 to 25 dpi (relapse phase), returning significant from 26 to 56 dpi (second remission, 26 dpi: p = .047; from 27 to 56 dpi: p < .01). Notably, the clinical profile of non-implanted rats was not significantly different from implanted animals (p = 0.324).

VEP latency in EAE rats

During each VEP recording session, we succeeded in obtaining a good signal-to-noise ratio, with N1 wave that was clearly distinguishable and measurable in terms of latency both in implanted (**Fig 5A**) and in non-implanted (**Fig 6A**) rats. In epidural-recorded EAE rats, mean N1 latencies were significantly increased at 13 dpi (p = .003), 20 dpi (p = .033), 27 dpi (p = .001) and 34 dpi (p = .0001) compared to epidural-recorded H rats . Moreover, epidural-recorded EAE rats showed a significant delay of N1 latency at 13 dpi (p = .020) and 34 dpi (p = .009) compared to their baseline (**Fig 5B**). In epidermal-recorded EAE rats, mean N1 latencies were significantly increased at 14 dpi (p < .0001), 21 dpi (p = .0001), 28 dpi (p = .00098) and 35 dpi (p < .0001) with respect to epidermal-recorded H rats. In addition, epidermal-recorded EAE rats presented a significant delay of N1 latency at 14 dpi (p = .0003), 21 dpi (p = .003), 28 dpi (p = .009) and 35 dpi (p = .001) compared to their baseline (**Fig 6B**). Interestingly, a remission was noticed at 42 dpi, with N1 latency that was no longer significantly increased (p = .258). This remission phase persisted until 56 dpi, where a significant delay in N1 latency was observed (p = .025).

Histology

At histological examination, H ONs of both implanted (**Fig 7A**) and non-implanted (**Fig 8A**) rats showed a regular structure, while EAE ONs of both implanted (**Fig 7B**) and non-implanted (**Fig 8B**) rats presented focally damaged areas. In particular, a significant increase of pathological areas was found in EAE ONs collected from implanted rats compared to H ONs (**Fig 7C**, p = .046). On the other hand, the quantitative increase of pathological areas found in EAE ONs dissected from non-implanted rats was not significant compared to H ONs (**Fig 8C**, p = .125).

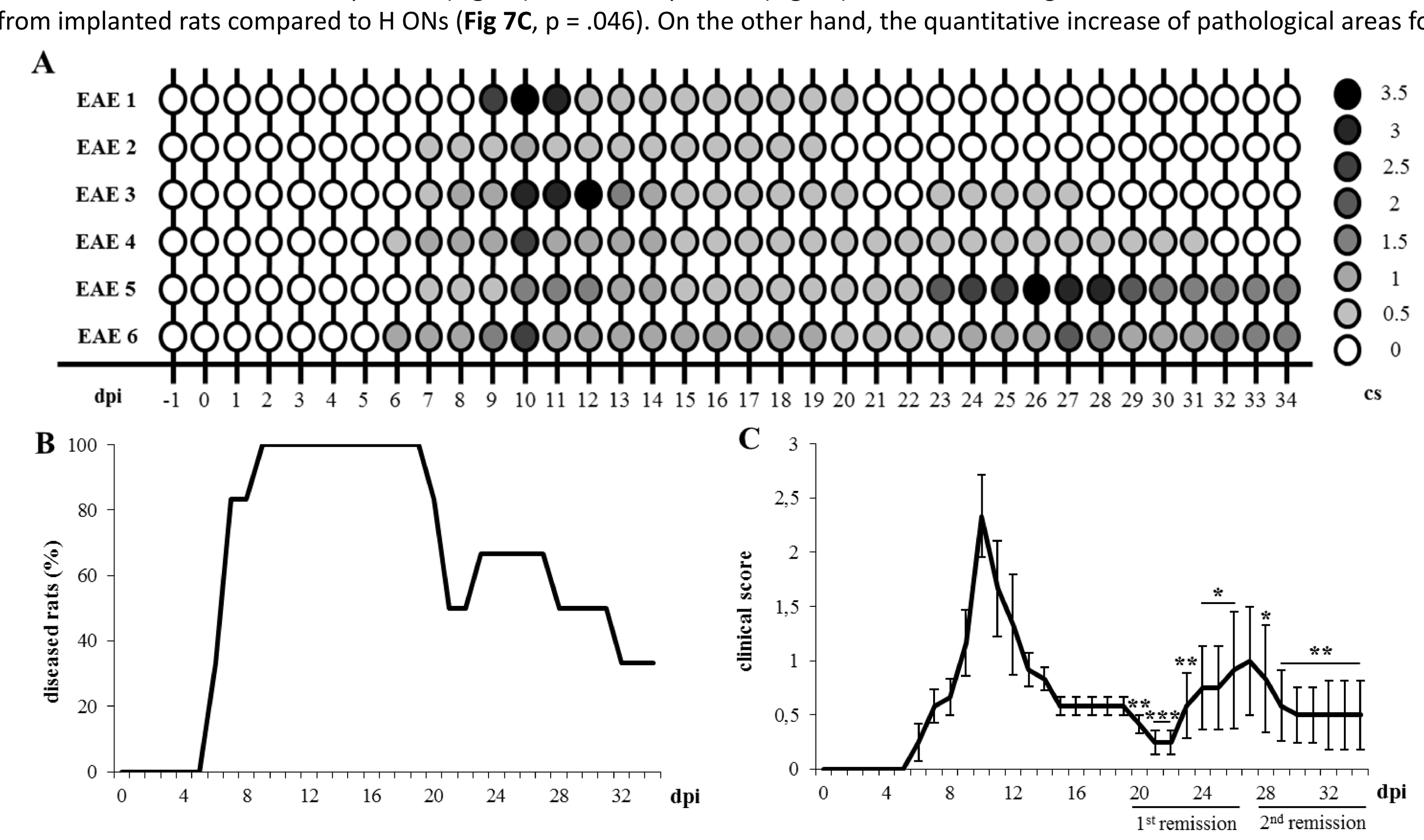

Figure 3. A. Graphic representation of individual clinical profile in implanted EAE rats from -1 to 34 dpi. **B.** Kaplan-Meier curve representing implanted EAE rats (n = 6) with clinical symptoms. **C.** Clinical score of implanted EAE rats (n = 6) from 0 to 34 dpi. Asterisks indicate significant changes compared with the first peak of the disease (10 dpi). *: p < .05; **: p < .01; ***: p < .001. Data are expressed as mean ± SEM.

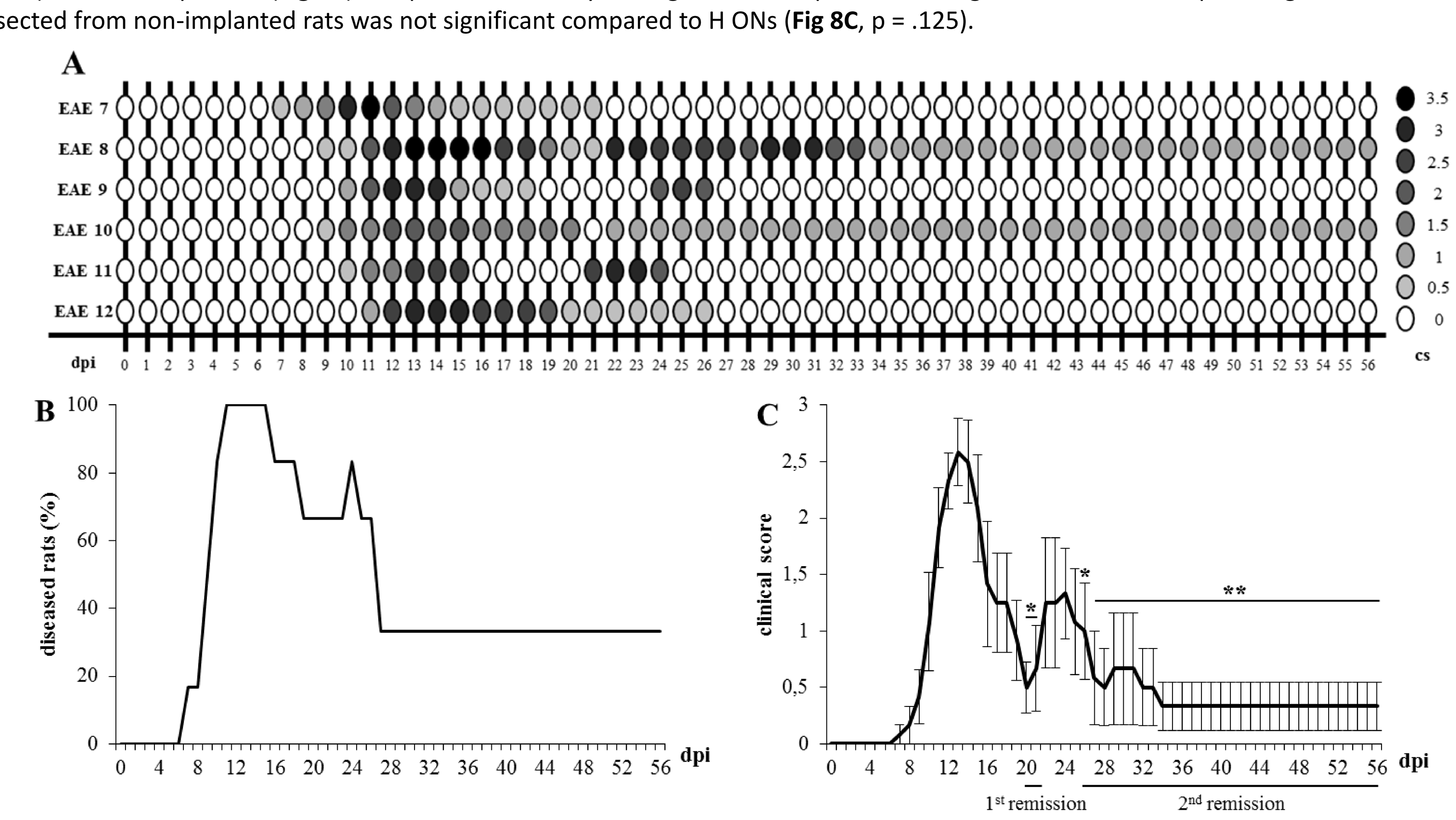

Figure 4. A. Graphic representation of individual clinical profile in non-implanted EAE rats from 0 to 56 dpi. **B.** Kaplan-Meier curve representing EAE rats (n = 6) with clinical symptoms. **C.** Clinical score of non-implanted EAE rats (n = 6) from 0 to 56 dpi. Asterisks indicate significant changes compared with the first peak of the disease (13 dpi). *: p < .05; **: p < .01. Data are expressed as mean ± SEM.

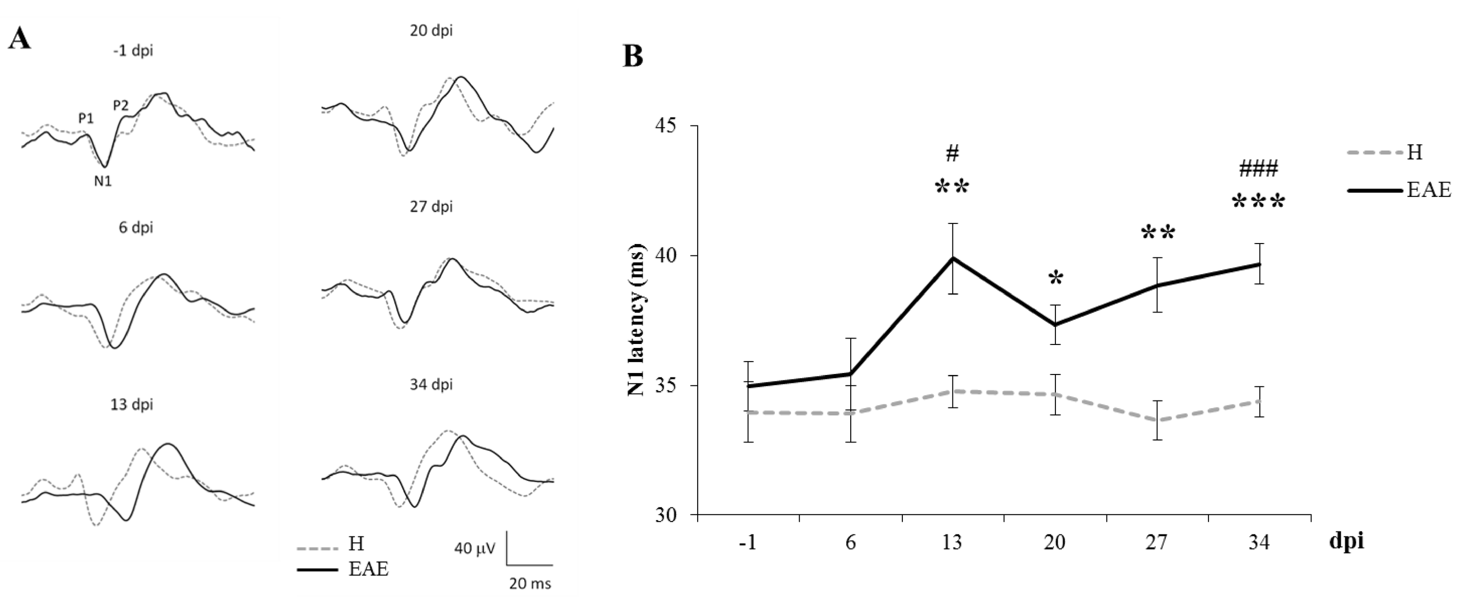

Figure 5. A. Representative VEP traces recorded with epidural electrodes from a H (dotted line) and an EAE (black line) rat at different time points, in which the P1-N1-P2 complex is highlighted. **B.** N1 latency of H (n = 8) and EAE (n = 6) implanted rats measured at different time points. Hashes indicate the significance level of VEPs measured in EAE rats compared to their baseline (#: p < .05; ###: p < .001). Asterisks indicate the significance level of VEPs recorded in EAE rats compared to the VEPs measured in H rats at the same time point (*: p < .05; **: p < .01; ***: p < .001). Data are expressed as mean ± SEM.

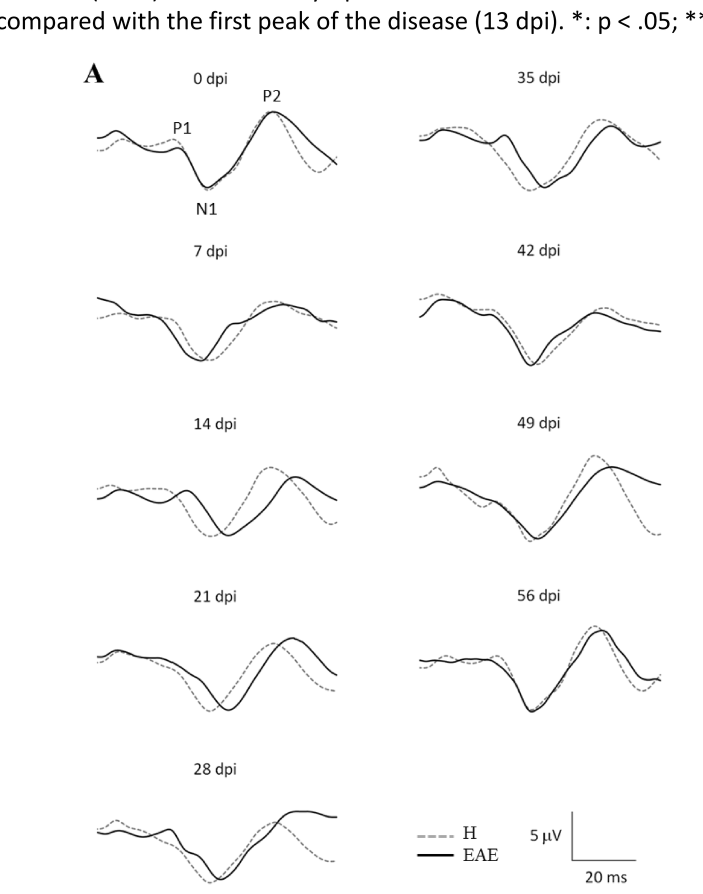

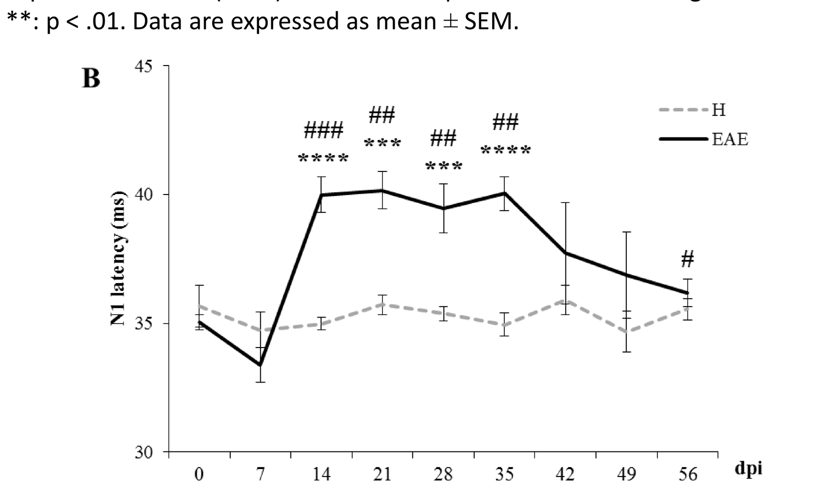

Figure 6. A. Representative VEP traces recorded with epidermal electrodes from a H (dotted line) and a EAE (black line) rat at different time points, in which the P1-N1-P2 complex is highlighted. **B.** N1 latency of H (n = 7) and EAE (n = 6) rats measured at different time points. Hashes indicate the significance level of VEPs measured in EAE rats compared to their baseline (#: p < .05; ##: p < .01; ###: p < .001). Asterisks indicate the significance level of VEPs recorded in EAE rats compared to the VEPs measured in H rats at the same time point (***: p < .001; ****: p < .0001). Data are expressed as mean ± SEM.

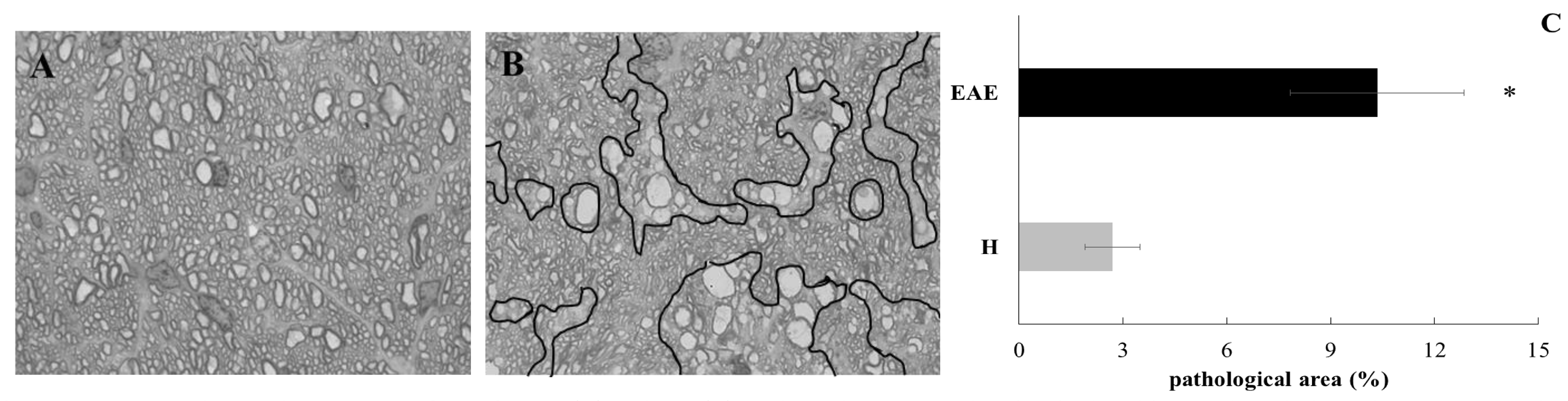

Figure 7. Transversal semi-thin sections of ONs from H (**A**) and EAE (**B**) implanted rats stained with toluidine-blue, with pathological areas surrounded by black lines (magnification: 100×). **C.** Quantification of pathological areas from H (n = 5) and EAE (n = 6) ON sections collected from implanted rats (*: p < .05). Data are expressed as mean ± SEM.

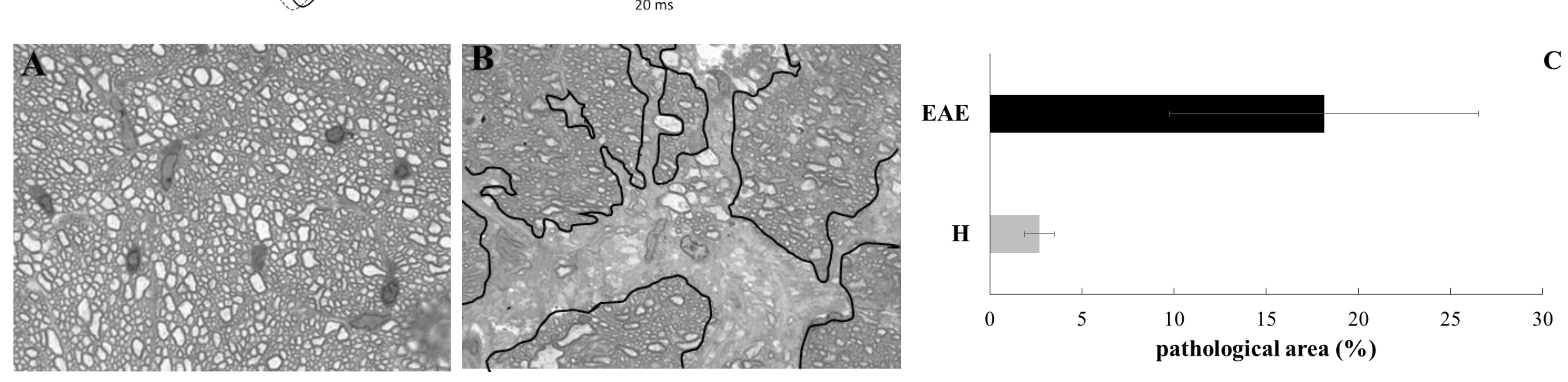

Figure 8. Transversal semi-thin sections of ONs from H (**A**) and EAE (**B**) non-implanted rats stained with toluidine-blue, with pathological areas surrounded by black lines (magnification: 100×). **C.** Quantification of pathological regions from H (n = 5) and EAE (n = 6) ON sections collected from non-implanted rats. Data are expressed as mean ± SEM.

Conclusions

Our findings confirmed the relapsing-remitting clinical course of the SCH-EAE DA rat model. Importantly, we showed clear ON dysfunctions in SCH-EAE, as VEP latencies were significantly delayed until the fifth week after immunization, along with pathological morphology detectable at histology. Subsequently, non-invasive VEP recording revealed an improvement of ON function, suggesting an endogenous recovery that could be due to a remyelination process[9]. Overall, further investigations will be necessary to elucidate the biological mechanisms involving ON demyelination/remyelination in SCH EAE. Finally, concerning our non-invasive recording method, novel drugs against MS optic neuritis could be tested in preclinical studies with a long-term monitoring of ON functionality. Therefore, the non-invasive VEP recording technique will allow a more accurate evaluation of risks and benefits of innovative treatments that could bring crucial improvements in MS clinical practice.

Bibliography & Acknowledgements

1. Lassmann H, Bradl M. Multiple sclerosis: experimental models and reality. Acta Neuropathol. 2017 Feb;133(2):223-244.
2. Robinson AP, Harp CT, Noronha A, Miller SD. The experimental autoimmune encephalomyelitis (EAE) model of MS: utility for understanding disease pathophysiology and treatment. Handb Clin Neurol. 2014;122:173-89.
3. Lorentzen JC, Issazadeh S, Storch M, Mustafa MI, Lassman H, Linington C, Klareskog L, Olsson T. Protracted, relapsing and demyelinating experimental autoimmune encephalomyelitis in DA rats immunized with syngeneic spinal cord and incomplete Freund's adjuvant. J Neuroimmunol. 1995 Dec 31;63(2):193-205.
4. Iglesias-Bregna D, Hanak S, Ji Z, Petty M, Liu L, Zhang D, McMonagle-Strucko K. Effects of prophylactic and therapeutic teriflunomide in transcranial magnetic stimulation-induced motor-evoked potentials in the dark agouti rat model of experimental autoimmune encephalomyelitis. J Pharmacol Exp Ther. 2013 Oct;347(1):203-11.
5. Jasse L, Vukusic S, Durand-Dubief F, Vartin C, Piras C, Bernard M, Pélisson D, Confavreux C, Vighetto A, Tilikete C. Persistent visual impairment in multiple sclerosis: prevalence, mechanisms and resulting disability. Mult Scler. 2013 Oct;19(12):1618-26.
6. You Y, Klistorner A, Thie J, Graham SL. Latency delay of visual evoked potential is a real measurement of demyelination in a rat model of optic neuritis. Invest Ophthalmol Vis Sci. 2011 Aug 29;52(9):6911-8.
7. Santangelo R, Castoldi V, D'Isa R, Marenna S, Huang SC, Cursi M, Comi G, Leocani L. Visual evoked potentials can be reliably recorded using noninvasive epidermal electrodes in the anesthetized rat. Doc Ophthalmol. 2018 Jun;136(3):165-175.
8. Onofrj M, Harnois C, Bodis-Wollner I. The hemispheric distribution of the transient rat VEP: a comparison of flash and pattern stimulation. Exp Brain Res. 1985;59(3):427-33
9. Castoldi V, Marenna S, Santangelo R, d'Isa R, Cursi M, Chaabane L, Quattrini A, Comi G, Leocani L. Optic nerve involvement in experimental autoimmune encephalomyelitis to homologous spinal cord homogenate immunization in the dark agouti rat. J Neuroimmunol. 2018 Sep 25;325:1-9.

This work was financially supported by Merck and by the Italian ministry of Education, University and Research (cluster project IVASCOMAR; CTN01_0177_165430)